Tailoring the release of encapsulated corrosion inhibitors from damaged coatings: Controlled release kinetics by overlapping diffusion fronts

E. Javierre[a,b,*], S.J. García[c], J.M.C. Mol[d], F.J. Vermolen[e], C. Vuik[e], S. van der Zwaag[c]

[a] Centro Universitario de la Defensa – AGM, Zaragoza, Spain
[b] Aragón Institute of Engineering Research (I3A), Universidad de Zaragoza, Zaragoza, Spain
[c] Novel Aerospace Materials, Delft University of Technology, Delft, The Netherlands
[d] Department of Materials Science and Engineering, Delft University of Technology, Delft, The Netherlands
[e] Delft Institute of Applied Mathematics, Delft University of Technology, Delft, The Netherlands

ARTICLE INFO

ABSTRACT

The goal of this work is to model the release of corrosion inhibitors from damaged organic coatings. In the present study, the healing response (i.e. the active corrosion protection) is triggered by the ingress of moisture in the coating through the walls of a damaged site, followed by the transport of the corrosion inhibitors to the exposed metal substrate by diffusion through the moisture present in the polymeric coating. We propose a mathematical–analytical model for each step of the healing response in order to determine, through computer simulation, the particle configurations that lead to desired regimes of inhibitors release into the damaged site. The used methodology is based on overlapping Fickian leaching kinetics of the individual corrosion inhibitor particles present in the coating. With the proposed model we analyze different release behaviors proportional to t^{α} with $0.25 < \alpha \leq 1$ reported in the literature. We study in detail the conditions yielding a linear release of corrosion inhibitors and determine the range of release rates that can be achieved as a function of the particle size distribution within the coating, the moisture diffusion through the coating and the capsule dissolution kinetics. In particular, we clearly demarcate the systems in which the linear release behavior cannot be obtained. Furthermore, we find that our model cannot predict the experimentally observed $t^{0.25}$ kinetics for any configuration and condition considered, which indicates that the release of inhibitor compounds from particle dissolution in these systems may not follow a Fickian behavior.

© 2012 Elsevier B.V. All rights reserved.

1. Introduction

Electrochemical corrosion of metals is a worldwide problem that entails high economic investments by governments and private users related to the protection of new metallic systems against corrosion as well as to the repair of damaged protective systems. One of the most common corrosion protection measures is the use of organic coating systems (mainly primer and top-coat) since they are both efficient, relatively cheap, and can be used in many different applications. Organic coating systems protect the metallic substrate via passive mechanisms (i.e. barrier against corrosive species and high adhesion to the metallic substrate), and active mechanisms (i.e. carriers of sacrificial pigments and corrosion inhibitors). When the active organic coating system is damaged and the metallic substrate exposed to the corrosive environment, the release of corrosion inhibitors from the primer to the exposed metal is activated. The most used corrosion inhibitor types are based on hexavalent chromium [1–4] which has demonstrated exceptional high performance in extending the longevity of corrosion protection of metals. Nevertheless, due to the known toxicity of Cr(VI) many other alternatives are being studied [5–9] among others with the help of recently developed high-throughput techniques for corrosion inhibitor selection and optimization [10–12].

Corrosion inhibitors may use different mechanisms to protect the exposed metal, although in most cases the protection starts with the ingress of water (or other triggering substance) through the breach in the coating towards the dispersed inhibitor particles, followed by the dissolution of the dispersed corrosion inhibitor particles, which will be transported to the exposed metallic surface through the same water path. The leaching rate of the corrosion inhibitors affects the immediate and long-term corrosion protection of the exposed metal and depends amongst others on temperature [13], polymer binder structural properties and pigment solubility [13,14], and pH [15,16].

In terms of corrosion protection, a desirable system would be one that releases corrosion inhibitors very fast during the initial

exposure time to offer a direct and immediate protection, but then very slowly and in a controlled manner. In this way, there will be a constant corrosion inhibitor supply without leading to the release of inhibitors that will not be able to react with the metallic surface and/or the formation of a depletion zone that is not able to keep the corrosion protection for long times. Experimental studies [17,18] have found that the leaching rate of chromates and other corrosion inhibitors depends on the polymeric matrix and the environment. Furman et al. [17] found that the release of chromates is not controlled by a Fickian diffusion process ($t^{0.5}$) but described by a faster $t^{0.25}$ release, whereas Nazarov [18] found that the leaching rate for the same corrosion inhibitor in a different matrix was closer to logarithmic release as for vanadate, while the release of phosphate was closer to the $t^{0.25}$ and the release of tungstate closer to a completely linear release (t^1). These different responses can be explained qualitatively on the basis of standard diffusion or dissolution being the rate determining steps. Putting aside the absolute amount of inhibitor released, these different time profiles indicate that there are different mechanisms, or at least different balances between mechanisms at work in the various cases. The different release trends for a single corrosion inhibitor from different polymer matrices can be explained by the physical and physicochemical interactions between the inhibitor and various functional groups in the polymeric matrix and the other fillers or corrosion inhibitor particles present in the coating. Another possible explanation for the different release trends could be the different pigment volume concentration – critical pigment volume concentration ratio (λ = PVC/CPVC) which depends on the corrosion inhibitor particles and the matrix and can have important effects on the corrosion protection of organic systems [19]. Moreover, these results show that a highly efficient corrosion inhibitor in a certain matrix can have an undesired release that reduces its efficiency in protecting against corrosion, while in other matrix the release trend can be more favorable. At the same time, a less efficient corrosion inhibitor could be incorporated into a polymeric matrix (coating) that promotes its efficiency in the fight against corrosion. As a consequence every corrosion inhibitor-organic matrix system has to be studied as a specific case. In order to gain some control in the otherwise unpredictable release rates as a function of the matrix and corrosion inhibitor and decrease the particle–matrix negative interactions, a different approach can be employed: the use of capsules, or coatings, covering the particles introduced in the polymer matrix. This approach could allow the coating designers to employ, independently of the polymeric matrix, the corrosion inhibitors they want with the desired release rate by modifying the employed capsules [20]. An appropriate understanding of the possible causes that make that a certain corrosion inhibitor in a certain matrix is released with a Fickian or non-Fickian diffusion rate will increase the necessary knowledge for the design of anticorrosive organic coatings with the desired release characteristics.

This paper contains a detailed theoretical model of the three stages of the response to damage in organic coatings (water ingress, capsule disintegration and inhibitor particle dissolution and diffusion to damage). The mathematical approach compiling the overall leaching behavior is used to give insights into the reasons (in terms of design parameters) behind the observed non-Fickian release of inhibitors from dispersed corrosion inhibitor particles. This work focuses on conditions yielding a linear release of encapsulated inhibitors, but the approach would be exactly the same for any other specified leaching behavior. The paper analyzes the effect of particle distribution in the matrix that gives a linear release in the absence of a chemical interaction of the corrosion inhibitor and capsule components with the polymeric matrix. The mathematical model in this paper highlights the big influence of the corrosion inhibitor particle distribution and concentration on the release kinetics and release trends.

2. Materials and methods

2.1. The mathematical model

The leaching behavior of inhibitors from organic matrices is modeled by coupling the sequential stages of the response to damage. The structure of a general organic coating, filled with an unspecified number of dispersed corrosion inhibitor particles is sketched in Fig. 1(a). It is assumed that the particles have a uniform rectangular geometry of homogeneous size, as is the case for chromate particles in epoxy polyamide matrices [21]. The corrosion protection of the metallic surface relies upon the dissolution of the inhibitor particles, activated by the ingress of moisture into the matrix, and the transport of their compounds to the damaged surface. To protect the inhibitors from reacting with the polymer matrix, thus affecting the leaching kinetics, the inhibitors may be encapsulated or isolated from the polymeric matrix by other means [20]. Under this assumption, the capsule should be opened in order to activate the leaching of the corrosion inhibitors. Thus, in the present model we incorporate in the primer corrosion inhibitor particles with a protective layer (e.g. capsule) that will be opened to allow the release of the corrosion inhibitors. In order to simplify the model and gain specific knowledge on how the basic stages influence the final leaching kinetics, the effect of the moisture absorption process from top to bottom (y axis) is not incorporated. Furthermore, assuming a sufficiently dispersed distribution of the inhibitor particles excludes soft-impingement effects and allows a study of the overall leaching kinetics as the superposition of the dissolution of the individual particles. A schematic representation of the three stages (i.e. moisture absorption, capsule disintegration and particle dissolution) involved in the response to damage for a single inhibitor particle is given in Fig. 1(b)), while the mathematical description of the processes taking place in each step is described below.

2.1.1. Moisture absorption

Moisture transport in polymeric matrices depends on the availability of molecular-sized pores in the polymer structure and on polymer–water affinity [23]. This interaction of water with the polymer chains is responsible for the anomalous diffusion of water within the coating [24]. However, moisture transport is well represented by Fickian diffusion in rubbery polymers (in which the polymer chain can quickly rearrange as the moisture front advances [25]) and in epoxy systems subject to relative humidities up to 75% [26]. Based on this, for our study case we assume that water ingress into the primer is described by Fick's second law

$$\frac{\partial u}{\partial t}(x, t) = \frac{\partial}{\partial x}\left(D_m \frac{\partial u}{\partial x}(x, t)\right) \quad \text{for} \quad x \in (0, d) \quad \text{and} \quad t > 0, \qquad (1)$$

where u denotes the moisture concentration, D_m the moisture diffusion rate along the polymer matrix, $x = 0$ the local coordinate of the capsule surface closest to the damage site and d its distance to the damage wall. The coating moisture saturation or equilibrium u_{sat}, which depends on relative humidity [26], is imposed at the scratch surface, that is

$$u(d, t) = u_{sat} \quad \text{for} \quad t > 0. \qquad (2)$$

We assume that the reaction activating either the dissolution of the protective capsule or, in its absence, the dissolution of the corrosion inhibitor particle occurs only when a threshold moisture level u_{min} is exceeded at the capsule (or particle) surface. This occurs at a certain time denoted by t_{cap}^{act}. Until this moment, the capsule
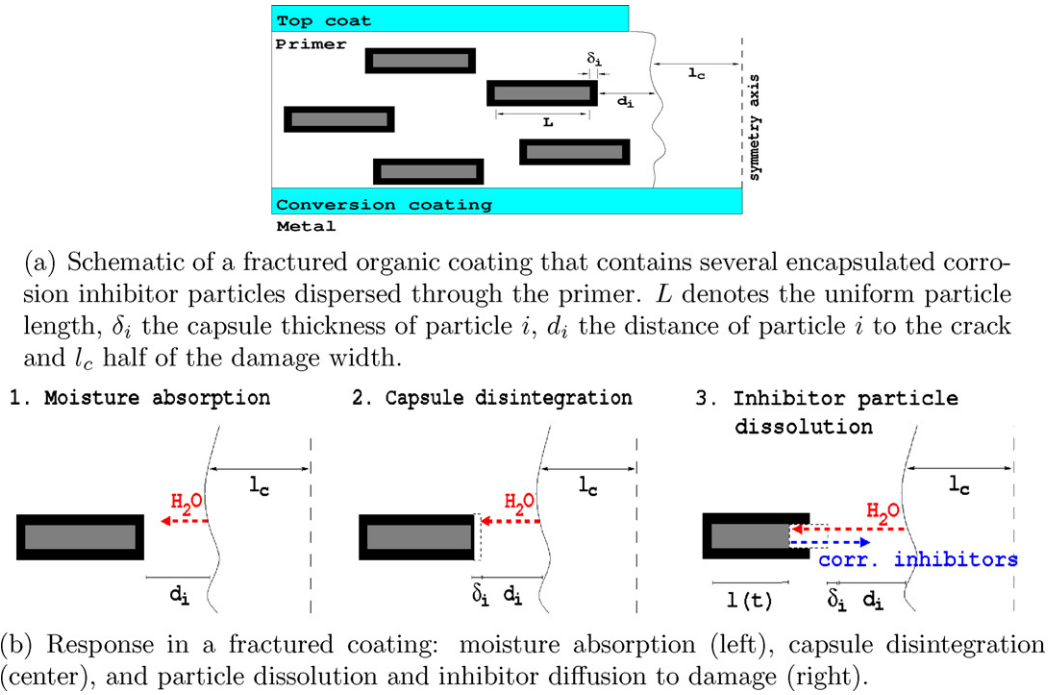
(a) Schematic of a fractured organic coating that contains several encapsulated corrosion inhibitor particles dispersed through the primer. L denotes the uniform particle length, δ_i the capsule thickness of particle i, d_i the distance of particle i to the crack and l_c half of the damage width.

(b) Response in a fractured coating: moisture absorption (left), capsule disintegration (center), and particle dissolution and inhibitor diffusion to damage (right).

Fig. 1. (a) Structure of an organic coating. (b) Phases in the response against corrosion in a fractured coating.

(or particle) surface blocks the advance of the moisture front, and hence

$$D_m \frac{\partial u}{\partial x}(0, t) = 0 \quad \text{for} \quad 0 < t < t_{cap}^{act}. \tag{3}$$

The simplicity of the geometries under study allows solving Eqs. (1)–(3) analytically. Thus, after separation of variables and algebraic manipulations we obtain that the moisture distribution through the coating until the dissolution of the capsule (or the particle, in absence of encapsulation) is activated (i.e. for $0 < t < t_{cap}^{act}$) is given by

$$u(x, t) = u_{sat} - \frac{4u_{sat}}{\pi} \sum_{n \geq 1} \frac{1}{2n-1} \sin(\frac{2n-1}{2d}\pi(d-x))e^{-((2n-1/2d)\pi)^2 D_m t}. \tag{4}$$

Of interest to our model is the value of t_{cap}^{act}. We obtain t_{cap}^{act} interpolating the moisture concentration at the capsule-matrix interface, $u(0, t)$, at the threshold moisture level u_{min}. As moisture advances as a diffusion front, the square root of t_{cap}^{act} is linearly related to the distance d, as can be seen in Fig. 2(a). Without loss of generality we can write this relation as

$$t_{cap}^{act} = \frac{1}{D_m}(\frac{d}{k})^2, \tag{5}$$

with k a dimensionless parameter depending only on the ratio u_{min}/u_{sat}. It shall be remarked here that no analytic expression has been found for k. Fig. 2(b) shows the values of k obtained from a parametric analysis using the above-described technique to find t_{cap}^{act} and using Eq. (5) to obtain k. Of course k is independent of D_m and d, and hence Fig. 2(b) gives a full characterization of k.

2.1.2. Disintegration of the capsule

In case of particle encapsulation, the membrane enclosing the particle must disintegrate (broken, in case of a propagating crack, or dissolved, in case of entering reactives degrading the matrix) to allow the leaching of the corrosion inhibitors. In this study, capsule dissolution is modelled as a phase transformation under equilibrium conditions at the capsule/polymer matrix interface [27]. From

a practical point of view, the capsule thickness (δ) shall be small in comparison to the particle size (L) or its distance to the center of the damage site ($d + l_c$, where l_c denotes half the damage width and d denotes the distance between the damage wall and the capsule surface), see Fig. 1. Hence, capsule dissolution can be accurately approximated by its self-similar solution [28,29]. The effect of the capsule components on the matrix properties is disregarded here, and only the dissolution time t_{cap}^{diss} is of interest for the determination of the inhibitors leaching kinetics. Following [28], we find that

$$t_{cap}^{diss} = \frac{1}{D_{cap}}(\frac{\delta}{\omega})^2, \tag{6}$$

where D_{cap} denotes the diffusion rate of the capsule compounds in moisture and ω is a dimensionless parameter which determines the capsule dissolution rate and depends only on the ratio between the capsule solubility in water, c_{cap}^{sol}, and the capsule concentration, c_{cap}^{part}, through the relation

$$\omega = 2 \frac{c_{cap}^{sol}}{c_{cap}^{sol} - c_{cap}^{part}} \frac{\exp(-\omega^2/4)}{\sqrt{\pi}[1 + \text{erf}(\omega/2)]} \tag{7}$$

(cf. Eq. (13) in [28], using $c^0 = 0$ as initially no capsule components are present in the primer and rearranging terms). In order to facilitate the visualization of this relation, ω has been plotted against $c_{cap}^{sol}/c_{cap}^{part}$ in Fig. 3.

2.1.3. Dissolution of the corrosion inhibitor particle

Once the barrier function of the capsule has been broken down, the corrosion inhibitor particle can also be dissolved. We assume that the reaction at the particle/bulk matrix interface driving particle dissolution is in equilibrium. This, together with the hypothesis of stoichiometric corrosion inhibitor particles, allows modeling the leaching of inhibitors into the polymeric matrix and the damage site as a binary Stefan problem [27]. The inhibitor
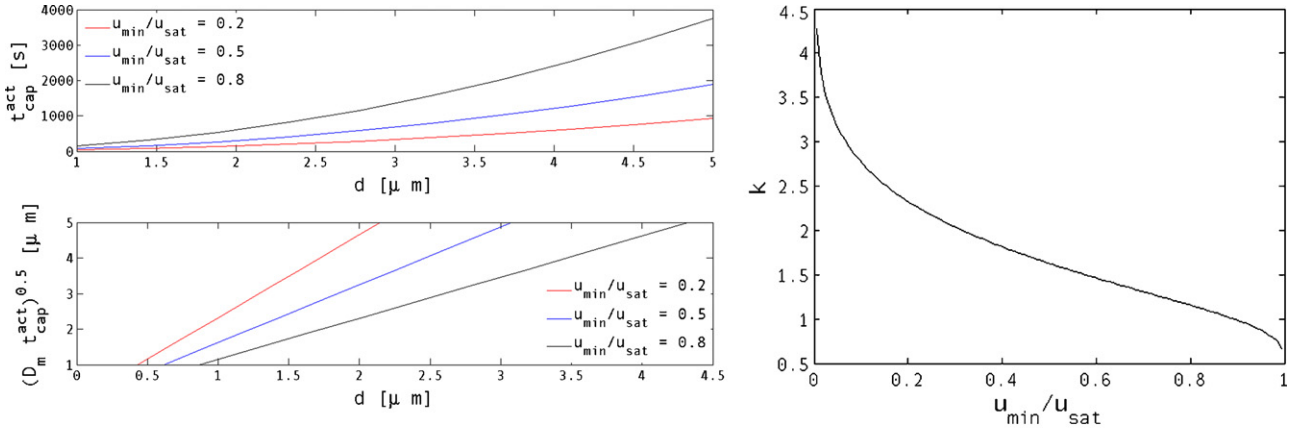
(a) t_{cap}^{act} (top) and $\sqrt{D_m t_{cap}^{act}}$ (bottom) as function of the distance d.

(b) Dependence of k on u_{min}/u_{sat}.

Fig. 2. Capsule disruption time and rate parameter k (taking $D_m = 5 \times 10^{-3} \, \mu m^2/s$).
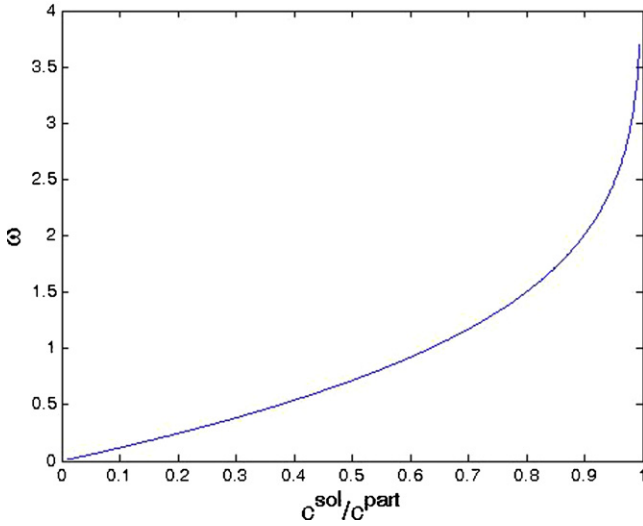

Fig. 3. Dependence of the dimensionless parameter ω on $c_{cap}^{sol}/c_{cap}^{part}$.

concentration c diffuses outside the particle through the moisture according to Fick's second law

$$\frac{\partial c}{\partial t}(x,t) = \frac{\partial}{\partial x}\left(D\frac{\partial c}{\partial x}(x,t)\right) \quad \text{for} \quad x \in (l(t), l_{end}) \quad \text{and} \quad t > 0, \tag{8}$$

where D denotes the inhibitor diffusion rate in moisture, $l(t)$ denotes the time dependent position of the particle/bulk matrix interface and l_{end} denotes the distance from the origin of the particle to the center of the damage site. For each particle in the coating we maintain a local coordinate system. In local coordinates, $x = 0$ denotes the origin of the particle (i.e. the furthest border to the scratch) and $x = L$ denotes the end of the particle (i.e. the closest border to the scratch). Under this notation $l_{end} = L + \delta + d + l_c$, see Fig. 1. Zero flux boundary conditions are applied, out of symmetry, at the center of the damage site, that is

$$D\frac{\partial c}{\partial x}(l_{end}, t) = 0 \quad \text{for} \quad t > 0. \tag{9}$$

Mass conservation drives the movement of the interface between the particle and the polymer matrix (i.e. the rate of particle dissolution), which is given by

$$(c^{part} - c^{sol})\frac{dl}{dt}(t) = D\frac{\partial c}{\partial x}(l(t), t) \quad \text{for} \quad t > 0, \tag{10}$$

where c^{part} denotes the inhibitor concentration within the particle and c^{sol} the maximum solubility of inhibitor in water, assuming that the dissolution of the inhibitor does not affect the spent volume.

We solve Eqs. (8)–(10) numerically using the so-called level set method [28]. With this approach we keep track of the particle–matrix interface position $l(t)$ in time as well as the particle concentration throughout the matrix and damage site. In order to determine the overall leaching kinetics we shall measure the amount of corrosion inhibitors released by a single particle to the damage site, which is given by

$$M^{crack}(t) = \int_0^{l_c} c(L + \delta + d + x, t)\,dx. \tag{11}$$

2.2. Controlled kinetics by overlapping diffusion fronts

For each particle in the primer, uniquely identified by its length L and its distance $\tilde{d}$ to the scratch (with $\tilde{d} = d + \delta$, δ the capsule thickness), we compute the time-history leached mass, $M^{crack}(t)$, as described above. Note that the curve $M^{crack}(t)$ does not incorporate the time needed for moisture to reach particle and dissolve the encapsulation. However, $M^{crack}(t)$ does incorporate the time t^{crack} needed for inhibitors from the particle to reach the crack void, see Fig. 4(a).

In order to obtain a desired leaking kinetics we must determine the times at which the different particles in the primer shall start dissolving. As we may be interested in different leaching kinetics (i.e. linear, Fickian or non-Fickian) we denote by $f(t)$ the desired leaching behavior without loss of generality. Denoting by θ_i the time lapses between the activation of consecutive particles, the overall leached mass is given by

$$M^{crack}(t) = \sum_{i=1}^{N} M_i^{crack}(t - \tilde{\theta}_i), \tag{12}$$

with $\tilde{\theta}_i = \sum_{j=1}^{i} \theta_j$ the activation time for particle i, see Fig. 4(b). For each particle configuration, we obtain the times $\theta_2, \theta_3, \ldots, \theta_N$ from a fitting procedure. The fitting is carried out in the time window that
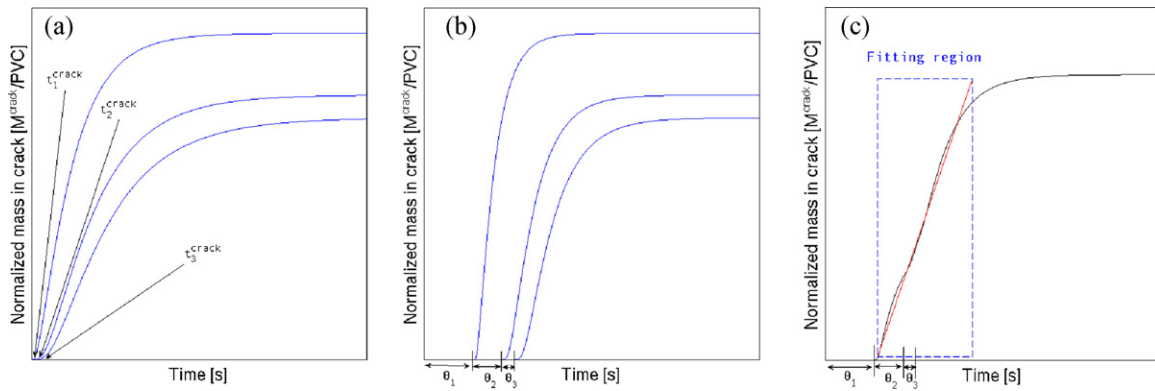
Fig. 4. (a) Time evolution of the mass released to the crack M^{crack} from three isolated particles located at increasing distances from the damage site. (b) Time evolution of the mass released to the crack when moisture absorption and capsule dissolution take for each particle θ_1, $\theta_1 + \theta_2$ and $\theta_1 + \theta_2 + \theta_3 s$ respectively. (c) Fit region and overall leaching kinetics determined by θ_1, θ_2 and θ_3.

covers the release from 1% to 90% of the total released mass. Consequently, θ_1 is a free parameter in the model that allows the user to shift backwards or forward the onset of leaching (see Fig. 4(c)). In this work, only the best fit to $f(t)$ is considered. Hence, $\theta_2, \theta_3, \ldots, \theta_N$ minimize the mean square error (MSE). We will say that a certain leaching behavior is accomplished when $R^2(\theta_2, \theta_3, \ldots, \theta_N) > 0.99$.

Once the activation times $\tilde{\theta}_i$ ($i = 1, \ldots, N$) are known, the primer moisture absorption and capsule dissolution kinetics can be determined. The activation times $\tilde{\theta}_i$ combine the time invested in moisture penetration from the scratch surface, t_{cap}^{act}, and the time invested in capsule dissolution, t_{cap}^{diss}. Hence, the following equations should hold:

$$\frac{1}{D_m}\left(\frac{d_i}{k}\right)^2 + \frac{1}{D_{cap}}\left(\frac{\delta_i}{\omega}\right)^2 = \tilde{\theta}_i, \quad \text{and} \quad d_i + \delta_i = \tilde{d}_i, \tag{13}$$

for $i = 1, \ldots, N$. Eq. (13) allow the user to define the range of moisture absorption and capsule dissolution kinetics ($D_m k^2$ and $D_{cap}\omega^2$ respectively) that yield the activation times $\tilde{\theta}_i$ and consequently the desired leaching behavior. If no further constrains are imposed, coatings fulfilling Eq. (13) shall verify

$$D_m k^2 > \max_{i=1,\ldots,N} \frac{\tilde{d}_i^2}{\tilde{\theta}_i} \quad \text{and} \quad D_{cap}\omega^2 < \min_{i=1,\ldots,N} \frac{\tilde{d}_i^2}{\tilde{\theta}_i} \tag{14a}$$

or

$$D_m k^2 < \max_{i=1,\ldots,N} \frac{\tilde{d}_i^2}{\tilde{\theta}_i} \quad \text{and} \quad D_{cap}\omega^2 > \min_{i=1,\ldots,N} \frac{\tilde{d}_i^2}{\tilde{\theta}_i} \tag{14b}$$

For each valid value of $D_m k^2$ and $D_{cap}\omega^2$ one unique solution exists for the distances d_i and δ_i ($i = 1, \ldots, N$). Once $D_m k^2$ and $D_{cap}w^2$ are fixed, the capsules thicknesses δ_i are obtained solving

$$\frac{(\tilde{d}_i - \delta_i)^2}{D_m k^2} + \frac{\delta_i^2}{D_{cap}\omega^2} = \tilde{\theta}_i,$$

whereas $d_i = \tilde{d}_i - \delta_i$ for $i = 1, \ldots, N$. If $D_m k^2$ and $D_{cap}\omega^2$ are taken according to Eq. (14b) then $d_i < \delta_i$. This solution could be rejected from a physical point of view, since the capsule thicknesses δ_i should be small compared with the other dimensions of the problem. If the user wants to further impose an upper bound of the capsules thicknesses, i.e. $\delta_i < \delta_{max}$ for $i = 1, \ldots, N$, then the coating moisture absorption and capsule dissolution kinetics must satisfy

$$D_m k^2 > \max_{i=1,\ldots,N} \frac{\tilde{d}_i^2}{\tilde{\theta}_i} \quad \text{and} \quad D_{cap}\omega^2 < \min_{i=1,\ldots,N} \frac{\delta_{max}^2}{\tilde{\theta}_i} \tag{14c}$$

It shall be noticed here that, in general, no valid solution can be obtained if the capsule thicknesses δ_i are fixed beforehand.

Hence, with the current analysis, for each particle distribution and each valid leaching kinetics we obtain a set of coating-capsule systems that yield the prescribed release behavior.

3. Results and discussion

3.1. Corrosion inhibitor release behavior: Fickian vs. non-Fickian

In order to understand why similar coatings with same inhibitor type present completely different release behaviors under similar conditions, the mathematical–analytical approach described in the previous section is employed. Under the current hypotheses, the dissolution of each individual particle follows a Fickian behavior, which is characterized by a proportionality relation between the mass released from the particle until time t and the square root of t. This linear relation is eventually lost (when around 80% of the particle mass is released, see Fig. 5(a)) to reach a plateau due to either the complete dissolution of the particle (as in the current case) or the cease of the dissolution process because of the saturation of the surrounding matrix.

However, when the dissolution of the N potentially active particles in the coating are combined in time, the resultant kinetics are, in principle, unpredictable, depending both on the particle configuration (size and position) and the matrix chemical properties. This is clearly visible in Fig. 5(b), where three different release kinetics are obtained for the same particle configuration but different activation times (θ). The chosen configuration, consisting of three particles of length $L = 5 \, \mu m$ located at distances $\tilde{d}_1 = 0.25$, $\tilde{d}_2 = 0.5$ and $\tilde{d}_3 = 1 \, \mu m$ from the scratch, serves as an illustrative example. We can impose a leaching kinetics proportional to $t^{0.5}$ (i.e. Fickian), $t^{0.75}$ and t by altering θ_2 and θ_3. The Fickian release behavior, the fastest of the three, is achieved for the smallest activation times ($\theta_2 = 0.0056$ and $\theta_3 = 0.0028$ s). The release behavior proportional for $t^{0.75}$ is obtained for the intermediate activation times ($\theta_2 = 1.1166$ and $\theta_3 = 3.7031$ s), whereas the linear release behavior, the slowest of the three, is reached for the largest activation times ($\theta_2 = 3.1737$ and $\theta_3 = 2.8377$ s).

The previous results show that the particle configuration alone cannot explain the different release trends. However, the coating moisture absorption and capsule dissolution kinetics cannot either. For each value of θ_1, inequalities Eqs. (14b) or (14c) determine the values that $D_m k^2$ and $D_{cap}\omega^2$ should have to yield the desired release kinetics. One can easily choose the same $D_m k^2$ and $D_{cap}\omega^2$ for the different release trends, which implies that the differences shall be explained by the capsule thicknesses δ_1, δ_2 and δ_3. For instance, $D_m k^2 = 1 \, \mu m^2/s$ and $D_{cap}\omega^2 = 10^{-2} \, \mu m^2/s$ fulfill Eq. (14c) for all particles and release kinetics if we take $\theta_1 = 1$ s and
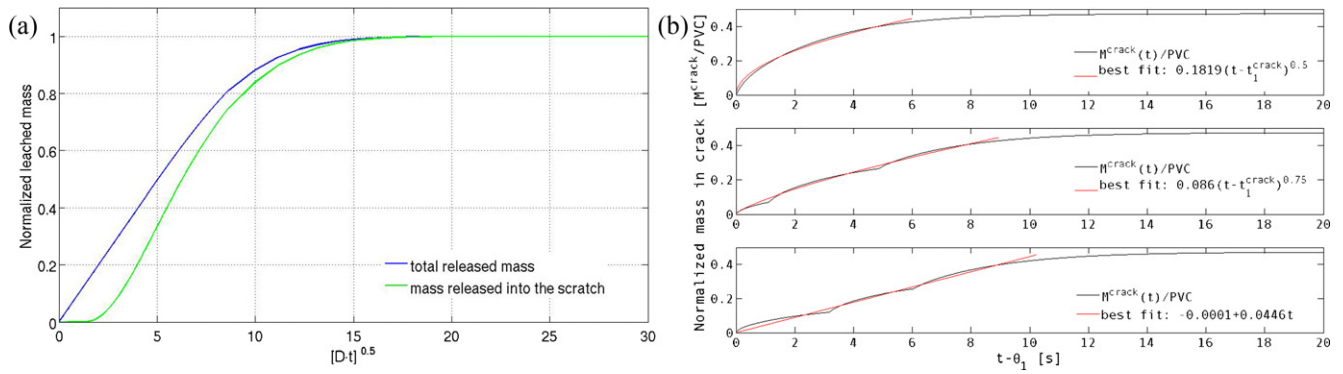
Fig. 5. (a) Release of mass from a single particle of length $L = 10\,\mu m$ located at a distance $\tilde{d} = 5\,\mu m$ from the damage site. (b) Leaching kinetics of a coating with three potentially active particles. In all cases $D = 5\,\mu m^2/s$.

Table 1
Activation times and capsule thicknesses for the three release kinetics under consideration taking $\theta_1 = 1\,s$, $\delta_{max} = 0.5\,\mu m$, $D_m k^2 = 1\,\mu m^2/s$ and $D_{cap}\omega^2 = 10^{-2}\,\mu m^2/s$. In all cases $D = 5\,\mu m^2/s$.

Release kinetics	$\tilde{\theta}_1$ (s)	δ_1 (μm)	$\tilde{\theta}_2$ (s)	δ_2 (μm)	$\tilde{\theta}_3$ (s)	δ_3 (μm)
$t^{0.5}$	1	0.0989	1.0056	0.0916	1.0085	0.0234
$t^{0.75}$	1	0.0989	2.1166	0.1410	5.8196	0.2286
t	1	0.0989	4.1737	0.2021	7.0114	0.2541

$\delta_{max} = 0.5\,\mu m$. Under these conditions, where moisture absorption is much faster than capsule dissolution, we observe that the capsule thicknesses should decrease with the particle distance to the scratch in order to obtain a Fickian behavior (see Table 1). However, for the linear release, the capsule thicknesses shall increase with the particle distance to the scratch. Note that in this particular example we have obtained the same δ_1 for the three release kinetics, which in general is not the case.

3.2. Linear release of corrosion inhibitors

In the remaining of this section we restrict our analysis to the targeted linear release of corrosion inhibitors from the coating matrix. Furthermore, to reduce the number of parameters involved, we consider only configurations with uniformly distributed particles. That is, we keep the interparticle distance d_p constant. Hence, $\tilde{d}_2 = \tilde{d}_1 + d_p, \tilde{d}_3 = \tilde{d}_1 + 2d_p$, etc. We study the effect of particle configuration on the amount of inhibitor concentration released to the crack and on the rate at which inhibitors are released.

In this work we consider configurations with a fixed pigment volume concentration (PVC) and vary the number of particles present in the coating matrix. Fig. 6 shows the particle density distribution as a function of the normalized distance between the crack and the closest particle $\tilde{d}_1/L$. Results show that for a fixed distance $\tilde{d}_1$, a linear release of inhibitors will be obtained only for configurations on which particles are spread along the coating matrix up to maximal interparticle distance d_p. Furthermore, the density function is increasing with the distance $\tilde{d}_1$ and with the number of particles in the system. That is, to maintain a linear release of inhibitors,

- the larger the separation between particles is, the further away the damage can occur, and
- the larger the particles are, the smaller the separation between particles must be.

The self healing capacity of the coating depends, among other factors, on the quantity of inhibitors released to the scratch and on the rate at which they are released. Fig. 7(a) shows the mass released into the scratch by the valid configurations previously

obtained. Results show that the mass in the scratch increases as the particles are located closer to it. Moreover, for sufficiently low interparticle distances, the amount of inhibitors in the scratch increases with the number of particles. Fig. 7(b) shows the release rate, derived from the linear fit parameters, for the valid configurations. We obtain that the rate at which inhibitors are released to the scratch increases with the number of particles in the coating. Furthermore, the fastest release is obtained when the scratch occurs close to a cluster of particles tightly distributed. Hence, in order to decide the optimal number of particles for a given coating system, the designer should find a compromise between the inhibitor mass necessary to stop corrosion on a typical scratch and the rate at which the inhibitors should be released.

3.3. Inhibitor release faster than Fickian

To conclude the analysis, we discuss the model predictions for release trends faster than Fickian. Several authors have reported leaching behaviors following a $t^{0.25}$ curve [17,18] for specific primers and corrosion inhibitors. Such behavior however could not be obtained by the proposed method and with the used particle
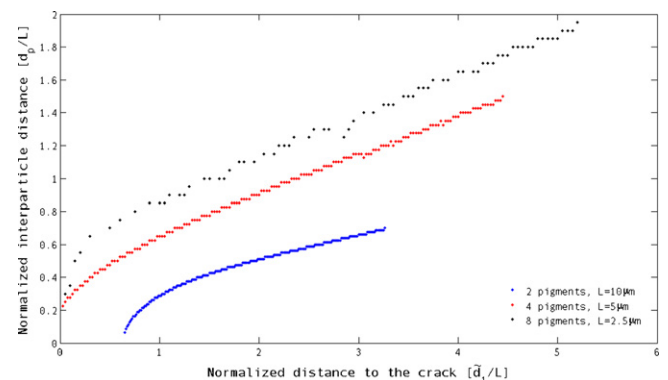

Fig. 6. Interparticle distance density function vs. the normalized distance to the scratch from the closest particle for a coating with 2, 4 and 8 particles enclosing the same PVC. Configurations bellow the curves yield a linear release of inhibitors. In all cases $D = 5\,\mu m^2/s$.
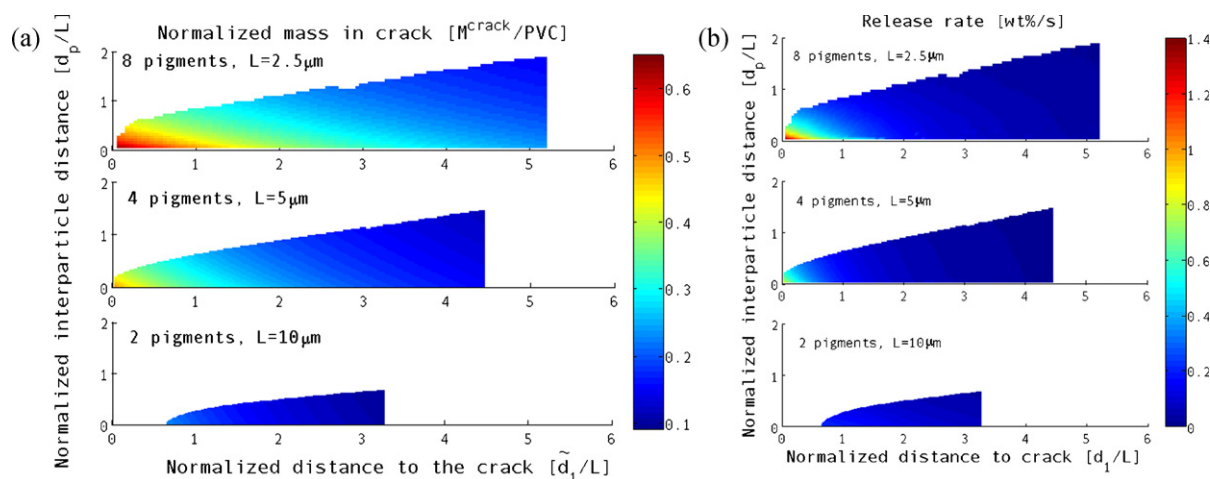
Fig. 7. (a) Normalized inhibitor mass in the scratch for the configurations with the same PVC and producing a linear release kinetics. (b) Release rate for the configurations with the same PVC and producing a linear release kinetics. In all cases $D = 5\,\mu m^2/s$.

numbers, lengths and overall accuracy, excluding the possibility that Fickian dissolution of particles can rule the observed leaching kinetics. Several possible reasons behind the faster-than-Fickian behavior were explored, without successful results. The overall leaching kinetics are determined basically from the activation times of the potentially active particles. Hence, Fickian moisture absorption or any other absorption kinetics that can be represented through an effective diffusion rate, are not expected to play an important role in the outcome. We also evaluated a non-linear diffusion of corrosion inhibitors through moisture [30], replacing Eq. (8) by

$$\frac{\partial c}{\partial t} = \nabla \cdot (Dc(1-c)\nabla c), \qquad (15)$$

but this change did not alter the results significantly (i.e. it only altered the slope of the release curve).

3.4. Mechanical factors influencing the release kinetics

This work is focused on the chemical response to damage. In this model, moisture ingress and inhibitor release are not altered by the mechanical condition of the coating. This simplification allows for a straightforward analysis of the role of particle configuration in the leaching kinetics. However, mechanical factors such as the coating matrix (micro)deformations, swealling of the coating layers and/or delamination will influence the transport kinetics of both moisture and inhibitor compounds. In fact, it is expected that some of the micropores in the matrix are closed while others are enlarged or new ones are created (microcracks) due to matrix deformation. A first work on the mechanical response of a damaged expansive coating has been recently published [31], and results demonstrate the large influence of the coating layers mechanical stiffness and adhesion in the self healing capacity of the coating. It is clear that efforts need to be focused on the development of multiscale mechano-chemical models coupling both inhibitor release and coating deformation. However, the development of such models needs to be associated with thoroughly designed experiments to determine realistic values of the parameters involved.

4. Conclusions

A mathematical model for the release of corrosion inhibitors from organic coatings is proposed in terms of the sequential absorption of moisture, encapsulation disruption and inhibitor

particle dissolution. Each of these processes is approximated by a physically justifiable but rather simple model, minimizing the number of parameters involved. The current paper focuses on linear release of corrosion inhibitors, although faster leaching behaviors have been characterized as well.

The results suggest that the release kinetics can only be explained when the inhibitor type and distribution, capsule system and coating matrix are considered as a whole. Changing one of these factors changes the overall leaching kinetics. Moreover, the obtained results give important insights into the optimal particle configuration for a given PVC. If the corrosion rate and the necessary inhibitor mass are well characterized as a function of the damage width, the coating designer can decide based on this model the optimal number and size of corrosion inhibitor particles to obtain the necessary leaching rate. Certainly, the presented model provides a qualitative explanation of the experimental findings reported in the literature [17,18]. However, a qualitative validation of the results can only be obtained if (among other aspects) the inhibitor particle distribution is known for the reported inhibitor-matrix systems. Steps are being taken in this direction to obtain a calibrated model in the near future.

Further extensions of the model, falling outside the scope of this paper but of our interest, include elucidating the dependence of the leaching kinetics on the PVC, the incorporation of inhibitor consuming corrosion reactions at the exposed substrate and the analysis of more realistic particle geometries.

References

[1] J. Sinko, Prog. Org. Coat. 42 (2001) 267.
[2] I.M. Baghni, S.B. Lyon, B. Ding, Surf. Coat. Technol. 185 (2004) 194.
[3] M.W. Kendig, R.G. Buchheit, Corrosion 59 (2003) 379.
[4] R.G. Buchheit, A.E. Hughes, Corr. Fundam. Test. Protect. 13A (2003) 720.
[5] A. von Koeppen, A.F. Pasowicz, B.A. Metz, Ind. Water Eng. 9 (1972) 25.
[6] H.B. Rudresh, S.M. Mayanna, Surf. Technol. 6 (1977) 139.
[7] R. LeRoy, Corrosion 34 (1978) 98.
[8] A.M. Beccaria, E.D. Mor, Br. Corr. J. 13 (1978) 186.

[9] D. Chadwick, T. Hashemi, Corr. Sci. 18 (1978) 39.

[10] B.D. Chamber, S.R. Taylor, M.W. Kendig, Corrosion 61 (2005) 480.

[11] P.A. White, A.E. Hughes, S.A. Furman, N. Sherman, P.A. Corrigan, M.A. Glenn, D. Lau, S.G. Hardin, T.G. Harvey, J. Mardel, T.H. Muster, S.J. Garcia, C. Kwakernaak, J.M.C. Mol, Corr. Sci. 51 (2009) 2279.

[12] T.H. Muster, A.E. Hughes, S.A. Furman, T. Harvey, N. Sherman, S. Hardin, P. Corrigan, D. Lau, F.H. Scholes, P.A. White, M. Glenn, J. Mardel, S.J. García, J.M.C. Mol, Electrochim. Acta 54 (2009) 3402.

[13] T. Prosek, D. Thierry, Prog. Org. Coat. 49 (2004) 209.

[14] R.L. Howard, I.M. Zin, J.D. Scantlebury, S.B. Lyon, Prog. Org. Coat. 37 (1999) 83.

[15] H. Wang, F. Presuel, R.G. Kelly, Electrochim. Acta 49 (2004) 239.

[16] I.M. Zin, R.L. Howard, S.J. Badger, J.D. Scantlebury, S.B. Lyon, Prog. Org. Coat. 33 (1998) 203.

[17] S.A. Furman, F.H. Scholes, A.E. Hughes, D. Lau, Prog. Org. Coat. 56 (2006) 33.

[18] A. Nazarov, D. Thierry, T. Prosek, N. Le Bozec, J. Electrochem. Soc. 152 B220 (2005).

[19] M.T. Rodríguez, S.J. García, J.J. Gracenea, K.A. Habib, J.J. Suay, Rev. Metal. (Madrid) Vol. Extr. (2005) 202.

[20] S.J. García, J.M.C. Mol, T.H. Muster, A.E. Hughes, J. Mardel, T. Miller, T. Markely, H. Terryn, J.H.W. de Wit, in: L. Fedrizzi (Ed.), Self-Healing Properties of New Surface Treatments, EFC-Wiley 58, 2011, p. 148.

[21] F.H. Scholes, S.A. Furman, A.E. Hughes, T. Nikpour, N. Wright, P.R. Curtis, C.M. Macrae, S. Intem, A.J. Hill, Prog. Org. Coat. 56 (2006) 23.

[23] M.R. Vanlandingham, R.F. Eduljee, J.W. Gillespie Jr., J. Appl. Polym. Sci. 71 (1999) 787.

[24] A.D. Drozdov, J.deC. Christiansen, R.K. Gupta, A.P. Shah, J. Polym. Sci. Part B: Polym. Phys. 41 (2003) 476.

[25] G.K. van der Wel, O.C.G. Adan, Prog. Org. Coat. 37 (1999) 1.

[26] M. Uschitsky, E. Suhir, J. Electron. Packag. 123 (2001) 47.

[27] F.J. Vermolen, E. Javierre, C. Vuik, L. Zhao, S. van der Zwaag, Comput. Mater. Sci. 39 (2007) 767.

[28] E. Javierre, C. Vuik, F.J. Vermolen, S. van der Zwaag, J. Comp. Appl. Math. 192 (2006) 445.

[29] J. Crank, Free and Moving Boundary Problems, Oxford University Press, 1984.

[30] J. Crank, The Mathematics of Diffusion, Oxford University Press, 1975.

[31] R. Rey, E. Javierre, S.J. Garca, S. van der Zwaag, J.M. Garca-Aznar, Surf. Coat. Technol. 206 (2012) 2220.